

A NEW CONSTITUTIVE MODEL FOR RUBBER-LIKE MATERIALS

Leonardo Hoss^a and Rogério J. Marczak^b

^a *Thoss Engenharia*

Rua Garibaldi, 559 / 202, Caxias do Sul, RS 95080-190, Brazil,

hoss.lhoss@yahoo.com.br

^b *Mechanical Eng. Dept. - Federal University of Rio Grande do Sul*

Rua Sarmento Leite 425, Porto Alegre, RS 90050-170, Brazil,

rato@mecanica.ufrgs.br

Keywords: Hyperelastic constitutive models, curve fitting, constitutive constants, material model calibration.

Abstract. The present work presents initially a study on the strain energy expressions for several constitutive models for incompressible elastomers published in the literature. Departing from a critical analysis of the key terms in the strain energy expressions of the models which show the best overall performance for incompressible rubbers, a new family of hyperelastic models is proposed. The proposed strain energy function keeps both, the terms responsible for capturing the stiffening under high strains, and the terms which represent the characteristic oscillation in the stress vs. strain curve under small strains. Results are presented for several strain regimes, and compared with other well known models.

1 INTRODUCTION

The principal point in modeling of a hyperelastic material is the correct selection of a constitutive relation. Most rubber-like materials presents the characteristic stress vs. strain curve, containing a softening behavior under small deformations, but rapidly stiffening as the range of deformation is increase. Nonetheless, many of the classical hyperelastic models fail to reproduce that behavior for all deformation regimes (Humphrey & Yin 1987, Humphrey 2003). This is one of the reasons for the proliferation of models proposed during the last two decades. Many of these models perform well in restricted ranges of deformation, or under a particular deformation mode, but very few can claim to be accurate up to strain magnitudes of 600-700%. And even when they are accurate for a given deformation mode, many fail in providing accurate predictions for other modes.

The present work studied in detail some relations available in the literature. In particular, their strain energy expressions were analyzed in order to investigate the contribution and role of each specific term. From this study a family of hyperelastic models for the analysis of elastomers and soft tissues is proposed.

2 CLASSICAL AND RECENT HYPERELASTIC MODELS

In most cases, strain energy functions can be written as a polynomial of the strain invariants $W = W(I_1, I_2, I_3)$, or directly in terms of the principal stretches $W = W(\lambda_1, \lambda_2, \lambda_3)$, where the compressibility is governed by the bulk modulus (K):

$$W = \underbrace{f(I_1, I_2, I_3, \dots)}_{\text{Incompressible part}} + \underbrace{g(K, \dots)}_{\text{Compressible part}} \quad (1)$$

In this work, the strain energy expressions are particularized for incompressible materials only ($I_3 = 1$), so that strain energy function takes the form $W = W(I_1, I_2)$. Table 1 presents the expressions of several well known models, as well as some newer contributions to the field, all particularized to the incompressible case. Table 1 also shows the calibration constants necessary for each model, obtained by fitting the equations with experimental data. These models form the base of the present study. They were implemented and calibrated against experimental data from uniaxial, shear, and biaxial testing for three material samples (Hoss, 2009).

3. GOODNESS OF FIT AND PREDICTION PERFORMANCE

The models in Tab.1 were assessed for following material data: Treloar's data (Jones & Treloar, 1975) and NR55 (Marczak *et al.*, 2006) for natural rubber, and MED4950 (Meier *et al.*, 2003) silicone. Due to the number of models analyzed and in order to make the analysis of the results (fitting and prediction) more objective, a grade system was used to perform a gross classification. Graphical results of all fits and predictions used here can be found in Hoss (2009). The grade system used to rank the hyperelastic models are based on the following rules:

- **Grade A:** Excellent overall performance, capturing faithfully the behavior of the engineering stress vs. strain ($t \times e$) curve for all three deformation modes (uniaxial, shear, and biaxial).

- Grade **B**: Good performance for the deformation mode used in the calibration. Not able to provide very good results for all deformation modes (predictions), or cannot fit well the experimental data for all ranges of deformation.
- Grade **C**: Good performance for the deformation mode used in the calibration, but poor results for the predictions.
- Grade **D**: Poor performance for all three deformation modes.
- Grade **E**: Faulty fits or erroneous predictions.

Since the experimental data were available for more than one deformation mode, uniaxial (T), pure shear (P), or biaxial (B), all models were calibrated for one test, but also verified regarding the quality of the theoretical predictions for the other tests.

3.1 Case Study: Natural Rubber – Larger deformations (Treloar’s data)

The deformation (e) ranges used for each test in this case were: $0 \leq e \leq 700\%$ for uniaxial tensile, $0 \leq e \leq 400\%$ for pure shear, and $0 \leq e \leq 350\%$ for biaxial tensile, respectively.

The grades assigned for each model are presented in Tab. 2, where the various hyperelastic models were grouped according to the type of strain energy function and kinship. The polynomial models (groups 1 and 2) provided erroneous predictions, showing an excessively rigid behavior. The models KI and HYI provided reasonable $t \times e$ curves while the other models in groups 3 and 4 delivered erroneous fits and predictions. The predictions of the models from groups 5 and 6 were disappointing, considering their potential after what is mentioned in the literature (Ogden, 1972; Bechir *et al.*, 2005). Group 7 provided excellent results when fitted for uniaxial tensile test, with exception of the YI2 model. The models YKI and AI from group 8 had convergence problems. The group 9, base of the family *limiting chain extensibility* had good performance, with exception of the THI model. The group 10, containing some promising models recently proposed to handle severe stiffening at very high strains, performed very well, except for the models G3I and CHGSI.

3.2 Case Study: Natural Rubber – Smaller deformations (NR55)

In order to assess the behavior of the hyperelastic models in deformation ranges distinct of the one studied in section 3.1, all models were re-analyzed against another sample of natural rubber (NR55 - Marczak, *et al.*, 2006). The ranges of deformations for each test were: $0 \leq e \leq 100\%$ for uniaxial tensile, $0 \leq e \leq 130\%$ for pure shear, and $0 \leq e \leq 70\%$ for biaxial tensile, respectively.

Model		Expression
Mooney-Rivlin (Rivlin & Saunders, 1951)	MRI_n	$W = \sum_{i+j=1}^3 C_{ij} (I_1 - 3)^i (I_2 - 3)^j$
Neo-Hookeano (Treloar., 1944)	NHI_n	$W = \frac{\mu}{2} (I_1 - 3)$
Gent-Thomas (Gent & Thomas, 1958)	GTI_n	$W = C_1 (I_1 - 3) + 3C_2 \ln(I_2)$
Hart-Smith, Improved (Hart-Smith, 1966)	HSAI	$W = \frac{C_1 e^{C_3 (I_1 - 3)^n}}{n} + 3C_2 \ln(I_2)$
Hart-Smith (Rozenwald, 1996)	HIS	$W = \frac{C_1 e^{C_3 (I_1 - 3)^2}}{2} + 3C_2 \ln(I_2)$
Fung (Fung, 1967)	FI	$W = \frac{\mu}{2b} (e^{b(I_1 - 3)} - 1)$
Veronda-Westmann (Veronda & Westmann, 1970)	VWI	$W = C_1 [e^{\alpha(I_1 - 3)} - 1] - C_2 [I_2 - 3]$
Ogden (Ogden, 1972)	OI_n	$W = \sum_{i=1}^N \frac{\mu_i}{\alpha_i} (\lambda_1^{\alpha_i} + \lambda_2^{\alpha_i} + \lambda_3^{\alpha_i} - 3)$
Peng-Landel (Peng & Landel, 1972)	PLI	$W = \sum_{i=1}^3 C_i (\lambda_i - 1 - \ln(\lambda_i)) - \frac{1}{6} \ln(\lambda_i)^2 + \frac{1}{18} \ln(\lambda_i)^3 - \frac{1}{216} \ln(\lambda_i)^4$
Knowles (Knowles, 1977)	KI	$W = \frac{\mu}{2b} \left(\left(1 + \frac{b(I_1 - 3)}{n} \right)^n - 1 \right)$
Kilian (Kilian, 1981)	KLI	$W = -\mu J_L \left[\ln \left(1 - \sqrt{\frac{I_1 - 3}{J_L}} \right) + \sqrt{\frac{I_1 - 3}{J_L}} \right]$
Van der Waals (Kilian, 1981)	VDWI	$W = \mu \left[-(\lambda_m^2 - 3)(\ln(1 - \eta) + \eta) - \frac{2}{3} a \left(\frac{1}{2} I_1 - \frac{3}{2} \right)^{3/2} \right],$ $\eta = \sqrt{\frac{I_1 - 3}{\lambda_m^2 - 3}} \quad I_1 = (1 - \beta)I_1 + \beta I_2$
Humphrey-Yin (Humphrey & Yin, 1987)	HYI	$W = C_1 (e^{C_2 (I_1 - 3)} - 1)$
Edwards-Vilgis (Edwards & Vigils, 1986)	EVI	$W = \frac{\mu}{2} \left[\frac{(J_L + 2)(J_L - 3)(I_1 - 3)}{J_L(J_L - I_1 + 3)} + \ln \left(1 - \frac{I_1 - 3}{J_L} \right) \right]$
Takamizawa-Hayashi (Takamizawa & Hayashi, 1987)	THI	$W = -c \ln \left[1 - \left(\frac{I_1 - 2}{J_L} \right)^2 \right]$
Yeoh (Yeoh, 1990)	YI_n	$W = \sum_{i=1}^N C_{i0} (I_1 - 3)^i$

Table 1. Common strain energy functions (W) for hyperelastic models (I_1 and I_2 are the first and the second strain invariants, respectively).

Model		Expression
Yeoh-Modified (Yeoh, 1993)	YMI	$W = C_{10}(I_1 - 3) + C_{20}(I_1 - 3)^2 + C_{30}(I_1 - 3)^3 + \frac{\alpha}{\beta}(1 - e^{-\beta(I_1 - 3)})$
Arruda-Boyce (Arruda & Boyce, 1993)	ABI5	$W = \mu \sum_{i=1}^N \frac{C_i}{\lambda_L^{2i-2}} (I_1^i - 3^i)$ $C_1 = \frac{1}{2}, C_2 = \frac{1}{20}, C_3 = \frac{11}{1050}, C_4 = \frac{19}{7050}, C_5 = \frac{519}{673750}$
Yamashita-Kawabata (Yamashita & Kawabata 1993)	YKI	$W = C_{10}(I_1 - 3) + \frac{C_3}{N+1}(I_1 - 3)^{N+1}$
Davis-De-Thomas (Davis <i>et al.</i> , 1994)	DDTI	$W = \frac{A}{2(1-n/2)} (I_1 - 3 + C^2)^{(1-n/2)} + k(I_1 - 3)^2$
Gent (Gent, 1996)	GI	$W = -\frac{\mu}{2}(I_L - 3) \ln \left[1 - \frac{I_1 - 3}{I_L - 3} \right]$
Gregory (Gregory <i>et al.</i> , 1997)	GYI	$W = \frac{A}{(2-n)} (I_1 - 3 + C^2)^{(1-n/2)} + \frac{B}{(2+m)} (I_1 - 3 + C^2)^{(1+m/2)}$
Yeoh-Fleming (Yeoh & Fleming, 1997)	YFI	$W = \frac{A}{B} [1 - e^{-B(I_1 - 3)}] - C_{10}(I_L - 3) \ln \left(1 - \frac{I_1 - 3}{I_L - 3} \right)$
Martins (Martins <i>et al.</i> , 1998)	MI	$W = C_1(e^{C_2(I_1 - 3)} - 1) + C_3(e^{C_4(\lambda_r - 1)^2} - 1)$
3 Parameters Gent (Gent, 1999)	G3I	$W = \frac{\mu}{2} \left[-\alpha(I_L - 3) \ln \left(1 - \frac{I_1 - 3}{I_L - 3} \right) + (1 - \alpha)(I_2 - 3) \right]$
Pucci-Saccomandi (Pucci & Saccomandi, 2002)	PSI	$W = -\frac{1}{2} \mu J_L \ln \left(1 - \frac{I_1 - 3}{J_L} \right) + C_2 \ln \left(\frac{1}{3} I_2 \right)$
Amin (Amin, <i>et al.</i> , 2002)	AI	$W = C_{10}(I_1 - 3) + \frac{C_3}{N+1}(I_1 - 3)^{N+1} + \frac{C_4}{M+1}(I_1 - 3)^{M+1}$
Hartmann-Neff (Hartmann & Neff, 2003)	HNI_n	$W = \alpha(I_1^3 - 3^3) + \sum_{i=1}^N C_{i0}(I_1 - 3)^i + \sum_{j=1}^M C_{0j}(I_2^{3/2} - 3\sqrt{3})^j$
Horgan-Saccomandi (Horgan & Saccomandi, 2004)	HGSI	$W = -\frac{\mu}{2} J_L \ln \left[\frac{(1 - (\lambda_1^2/J_L))(1 - (\lambda_2^2/J_L))(1 - (\lambda_3^2/J_L))}{(1 - (1/J_L))^3} \right]$
Bechir (Bechir <i>et al.</i> , 2006)	BI_n	$W = \sum_{n=1}^{\infty} \sum_{r=1}^{\infty} C_n^r (\lambda_1^{2n} + \lambda_2^{2n} + \lambda_3^{2n} - 3)^r$
Polynomial	PI3	$W = \sum_{i+j=1}^N C_{ij} (I_1 - 3)^i (I_2 - 3)^j$

Table 1. Hyperelastic models (cont'd).

The results are presented in Tab. 3. It is worth to mention that the literature usually claims that the best calibrations are obtained when the models are fitted with biaxial data. The results of Tab.3 are confirming what was found also in the results of Tab.2, that the best results were obtained when the models were fitted with uniaxial data, contradicting what is generally found in the literature. It was also found that all polynomial models of the groups 1 and 2 presents excessively rigid predictions for deformation modes other than the one used in the calibration.

The members of the groups 4 and 9 delivered similar behaviors, not providing good results for all tests or all deformation ranges analyzed. The best results were obtained by the YI3, YI5 models in group 7. The remaining models from the other groups did not presented good performance. Surprisingly, the PSI model did not performed well for these smaller deformation ranges, unlike what was found to the fitting make using the Treloar's data doesn't have good performance.

3.3 Case Study: Silicone Rubber (MED4950)

For this material, the deformation ranges for each test were (Meier *et al.*, 2003): $0 \leq e \leq 600\%$ for uniaxial tensile, and $0 \leq e \leq 300\%$ for biaxial tensile, respectively. Data for shear test were not available.

As a general rule, the groups 1 and 2, in spite of fitting well the curve $t \times e$ for all calibration tests, exhibited excessively rigid predictions for tests different of the one used in the calibration. Except for the KI and HYI models, the members of the groups 3 to 6 did not presented good performance. This particular case study indicated the potential of the power *law* models. All models containing these terms in their strain energy expression were able to follow the stress-stiffening effect in high strain ranges.

The models YI2, YI3, YI5, YKI and GYI from the groups 7 and 8 showed excellent results, while the YFI model was the only model in group 10 to present good performance.

4. THE PROPOSED MODELS

The family of models HMI was a development of the authors aiming to generalize a strain energy expression that could be applicable to a wide range of elastomers and organic tissues. A secondary, but not less important objective was to include all necessary terms in the strain energy expression in such a way that the characteristic shapes of the $t \times e$ curves could be captured faithfully in both, small and large deformation range. In essence, it is a heuristic model generated under the observation of performance of the models discussed in the previous sections. The basic idea was keep the terms in the expression of W that could reproduce the softening behavior at moderate strains and stiffening characteristic of large strains as well. These terms were identified in the various hyperelastic models studied by observing the common functions present in the models clearly performing well in fitting and predicting the desired behaviors. Two models are proposed. The first one, called HMLSI, was developed specially to capture the stiffness oscillation during the first stages of the stress vs. strain curve, typically $0 \leq e \leq 100\%$:

Group	Model	Calibration		
		<i>T</i>	<i>P</i>	<i>B</i>
GROUP ₁	MRI2	<i>E</i>	<i>B</i>	<i>B</i>
	MRI3	<i>D</i>	<i>B</i>	<i>C</i>
	MRI5	<i>C</i>	<i>D</i>	<i>C</i>
	MRI9	<i>C</i>	<i>C</i>	<i>C</i>
GROUP ₂	HNI1	<i>C</i>	<i>C</i>	<i>C</i>
	HNI2	<i>C</i>	<i>C</i>	<i>C</i>
	HNI3	<i>C</i>	<i>E</i>	<i>E</i>
	PI3	<i>C</i>	<i>C</i>	<i>C</i>
GROUP ₃	NHI	<i>E</i>	<i>D</i>	<i>D</i>
	GTI	<i>E</i>	<i>D</i>	<i>D</i>
	HSAI	<i>B</i>	<i>E</i>	<i>E</i>
	HSI	<i>E</i>	<i>E</i>	<i>E</i>
GROUP ₄	FI	<i>D</i>	<i>D</i>	<i>D</i>
	VWI	<i>D</i>	<i>D</i>	<i>E</i>
	KI	<i>B</i>	<i>D</i>	<i>B</i>
	HYI	<i>B</i>	<i>D</i>	<i>B</i>
GROUP ₅	OI2	<i>B</i>	<i>B</i>	<i>B</i>
	OI3	<i>D</i>	<i>C</i>	<i>C</i>
	BI2	<i>B</i>	<i>D</i>	<i>E</i>
	BI3	<i>D</i>	<i>D</i>	<i>E</i>

Group	Model	Calibration		
		<i>T</i>	<i>P</i>	<i>B</i>
GROUP ₆	PLI	<i>E</i>	<i>E</i>	<i>E</i>
	MI	<i>D</i>	<i>B</i>	<i>C</i>
	KLI	<i>E</i>	<i>D</i>	<i>B</i>
	VDWI	<i>C</i>	<i>E</i>	<i>D</i>
GROUP ₇	YI2	<i>B</i>	<i>D</i>	<i>B</i>
	YI3	<i>A</i>	<i>A</i>	<i>A</i>
	YI5	<i>A</i>	<i>B</i>	<i>A</i>
	YMI	<i>A</i>	<i>D</i>	<i>A</i>
GROUP ₈	YKI	<i>A</i>	<i>D</i>	<i>B</i>
	AI	<i>A</i>	<i>D</i>	<i>B</i>
	DDTI	<i>D</i>	<i>E</i>	<i>E</i>
	GYI	<i>B</i>	<i>D</i>	<i>D</i>
GROUP ₉	THI	<i>E</i>	<i>E</i>	<i>E</i>
	EVI	<i>B</i>	<i>D</i>	<i>B</i>
	ABI5	<i>B</i>	<i>D</i>	<i>B</i>
	GI	<i>B</i>	<i>D</i>	<i>B</i>
GROUP ₁₀	YFI	<i>A</i>	<i>A</i>	<i>B</i>
	G3I	<i>C</i>	<i>E</i>	<i>C</i>
	PSI	<i>A</i>	<i>A</i>	<i>B</i>
	HGSI	<i>B</i>	<i>D</i>	<i>C</i>

Table 2. Natural Rubber (Treloar’s data). Data for fitting: T ($0 \leq e \leq 700\%$), P ($0 \leq e \leq 400\%$), B ($0 \leq e \leq 350\%$).

Group	Model	Calibration		
		<i>T</i>	<i>P</i>	<i>B</i>
GROUP ₁	MRI2	<i>D</i>	<i>D</i>	<i>D</i>
	MRI3	<i>C</i>	<i>E</i>	<i>C</i>
	MRI5	<i>C</i>	<i>E</i>	<i>C</i>
	MRI9	<i>C</i>	<i>C</i>	<i>C</i>
GROUP ₂	HNI1	<i>C</i>	<i>C</i>	<i>C</i>
	HNI2	<i>C</i>	<i>C</i>	<i>C</i>
	HNI3	<i>C</i>	<i>C</i>	<i>C</i>
	PI3	<i>C</i>	<i>C</i>	<i>C</i>
GROUP ₃	NHI	<i>B</i>	<i>D</i>	<i>D</i>
	GTI	<i>B</i>	<i>E</i>	<i>C</i>
	HSAI	<i>E</i>	<i>E</i>	<i>E</i>
	HSI	<i>C</i>	<i>D</i>	<i>C</i>
GROUP ₄	FI	<i>D</i>	<i>D</i>	<i>E</i>
	VWI	<i>D</i>	<i>D</i>	<i>C</i>
	KI	<i>B</i>	<i>D</i>	<i>D</i>
	HYI	<i>B</i>	<i>D</i>	<i>D</i>
GROUP ₅	OI2	<i>D</i>	<i>B</i>	<i>C</i>
	OI3	<i>C</i>	<i>D</i>	<i>D</i>
	BI2	<i>C</i>	<i>C</i>	<i>E</i>
	BI3	<i>C</i>	<i>C</i>	<i>E</i>

Group	Model	Calibration		
		<i>T</i>	<i>P</i>	<i>B</i>
GROUP ₆	PLI	<i>D</i>	<i>E</i>	<i>E</i>
	MI	<i>B</i>	<i>B</i>	<i>E</i>
	KLI	<i>D</i>	<i>D</i>	<i>D</i>
	VDWI	<i>E</i>	<i>E</i>	<i>E</i>
GROUP ₇	YI2	<i>B</i>	<i>D</i>	<i>B</i>
	YI3	<i>A</i>	<i>A</i>	<i>A</i>
	YI5	<i>A</i>	<i>A</i>	<i>A</i>
	YMI	<i>A</i>	<i>E</i>	<i>E</i>
GROUP ₈	YKI	<i>B</i>	<i>A</i>	<i>B</i>
	AI	<i>A</i>	<i>B</i>	<i>A</i>
	DDTI	<i>E</i>	<i>D</i>	<i>D</i>
	GYI	<i>A</i>	<i>A</i>	<i>B</i>
GROUP ₉	THI	<i>E</i>	<i>E</i>	<i>E</i>
	EVI	<i>B</i>	<i>D</i>	<i>D</i>
	ABI5	<i>B</i>	<i>D</i>	<i>D</i>
	GI	<i>B</i>	<i>D</i>	<i>D</i>
GROUP ₁₀	YFI	<i>A</i>	<i>D</i>	<i>A</i>
	G3I	<i>C</i>	<i>C</i>	<i>D</i>
	PSI	<i>C</i>	<i>C</i>	<i>C</i>
	HGSI	<i>B</i>	<i>D</i>	<i>C</i>

Table 3. Natural Rubber (NR55). Data for fitting: T ($0 \leq e \leq 100\%$), P ($0 \leq e \leq 130\%$), B ($0 \leq e \leq 70\%$).

Group	Model	Calibration		Group	Model	Calibration	
		<i>T</i>	<i>B</i>			<i>T</i>	<i>B</i>
GROUP ₁	MRI2	<i>E</i>	<i>C</i>	GROUP ₆	PLI	<i>E</i>	<i>E</i>
	MRI3	<i>C</i>	<i>C</i>		MI	<i>C</i>	<i>C</i>
	MRI5	<i>C</i>	<i>C</i>		KLI	<i>C</i>	<i>C</i>
	MRI9	<i>C</i>	<i>C</i>		VDWI	<i>C</i>	<i>E</i>
GROUP ₂	HNI1	<i>C</i>	<i>C</i>	GROUP ₇	YI2	<i>A</i>	<i>B</i>
	HNI2	<i>C</i>	<i>C</i>		YI3	<i>A</i>	<i>B</i>
	HNI3	<i>C</i>	<i>D</i>		YI5	<i>A</i>	<i>D</i>
	PI3	<i>C</i>	<i>C</i>		YMI	<i>E</i>	<i>B</i>
GROUP ₃	NHI	<i>D</i>	<i>D</i>	GROUP ₈	YKI	<i>A</i>	<i>B</i>
	GTI	<i>E</i>	<i>D</i>		AI	<i>D</i>	<i>D</i>
	HSAI	<i>C</i>	<i>E</i>		DDTI	<i>E</i>	<i>E</i>
	HSI	<i>E</i>	<i>D</i>		GYI	<i>A</i>	<i>B</i>
GROUP ₄	FI	<i>D</i>	<i>D</i>	GROUP ₉	THI	<i>E</i>	<i>E</i>
	VWI	<i>C</i>	<i>E</i>		EVI	<i>B</i>	<i>B</i>
	KI	<i>A</i>	<i>B</i>		ABI5	<i>B</i>	<i>B</i>
	HYI	<i>B</i>	<i>B</i>		GI	<i>B</i>	<i>B</i>
GROUP ₅	OI2	<i>B</i>	<i>C</i>	GROUP ₁₀	YFI	<i>A</i>	<i>B</i>
	OI3	<i>C</i>	<i>C</i>		G3I	<i>C</i>	<i>C</i>
	BI2	<i>C</i>	<i>E</i>		PSI	<i>E</i>	<i>B</i>
	BI3	<i>C</i>	<i>E</i>		HGSI	<i>B</i>	<i>C</i>

Table 4. Silicone Rubber (MED55). Data for fitting: T ($0 \leq e \leq 600\%$), B ($0 \leq e \leq 300\%$).

- **HMLSI** (HM Low Strain Incompressible).

The HMLSI model has a hybrid formulation, since it consists in the addition of an exponential term to the basic power-law model of Knowles (1977), responsible for improving the quality of fits and predictions at small strains (Yeoh, 1993). Its strain energy expression is based on the first strain invariant, only, and is fairly general since it allows particularization to simpler models:

$$W = \frac{\alpha}{\beta} (1 - e^{-\beta(I_1-3)}) + \frac{\mu}{2b} \left(\left(1 + \frac{b(I_1-3)}{n} \right)^n - 1 \right) \quad (2)$$

where α , β , μ , b , n and C_2 are the material constants. For the case $\alpha = 0$ the KI model is obtained, while taking the limit $n \rightarrow \infty$ in Eq. (2) results in the FI model.

The second variation of the proposed model is an evolution of Eq.(2), where terms responsible for capturing the stiffening at high strains were added. It is aimed to perform well for all ranges of deformation:

- **HMHSI** (HM High Strain Incompressible)

The main difference of this model to the HMLSI model is in consideration of the second strain invariant in the strain energy expression. This is the term found responsible for providing a better sensitivity to the rapid stiffening at moderate and large stretches. The exponential term of Eq.(2) was not dropped, though, in order to keep the good prediction capabilities of the

HMLSI model under small strains. The final expression for W therefore considers both strain invariants:

$$W = \frac{\alpha}{\beta}(1 - e^{-\beta(I_1-3)}) + \frac{\mu}{2b} \left(\left(1 + \frac{b(I_1-3)}{n}\right)^n - 1 \right) + C_2 \ln\left(\frac{1}{3} I_2\right) \quad (3)$$

where α , β , μ , b , n and C_2 represent the constitutive constants. The KI model is obtained by $\alpha = C_2 = 0$ in Eq. (3), while the limit $n \rightarrow \infty$ along with $\alpha = C_2 = 0$ reduces Eq. (3) to the FI model.

The dominant base function in Eq.(3) is still the same of the KI model, so that it can be considered a *power-law* model. This is not a coincidence, since the KI model not only shows good results as discussed in section 3, but also because it is one of the precursors in trying to capture the stiffening at large strains. The terms added to the original function are responsible for adjusting the power-law term to better reproduce the aforementioned stiffness changes. The exponential term confers better fit in small strains as in Eq.(2), and it was chosen from the analysis of the fitting and prediction capabilities of the YFI model, which has a similar formulation. The logarithmic term was employed due to the excellent results obtained by the PSI model in large strain regime.

5. ASSESSMENT OF THE PROPOSED MODEL

In this section the proposed model is tested with the same material samples and deformation ranges analyzed in the section 3. This assessment is based on a non-linear correlation coefficient (r^2) between the experimental and theoretical curves proposed by Hoss (2009), suitable for non-linear curve fitting. The results obtained with the proposed model are compared against the YMI, YFI and PSI models because these are the ones with closest resemblance to the HM models, and therefore provide an interesting ground to check for the differences between them.

5.1. Case Study: Natural Rubber – Large Deformations (Treloar’s data)

The YMI, YFI, PSI and HMHSI models were fitted for the uniaxial tensile test in $0 \leq e \leq 700\%$. Figure 1 clearly shows that the HMHSI model adjust well all ranges of deformation, producing predictions very similar to the PSI model (which is considered a reference in capturing the stiffening effect). Figure 1 also shows that the models YMI and YFI have a poorer performance for predicting the biaxial behavior. In Fig. 2 one can compare the predictions (continuous lines) of the proposed model and the KI model with experimental results (dashed lines) for all three deformation modes, uniaxial (black), pure shear (blue), and biaxial (red).

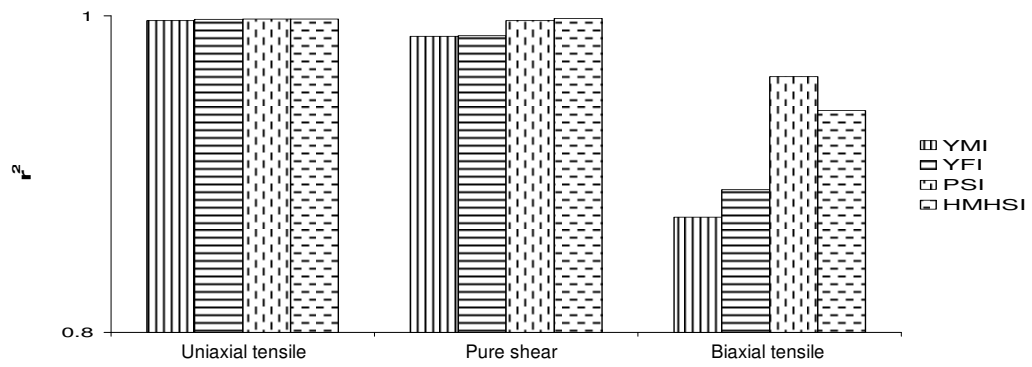


Figure 1. Natural Rubber (Treloar’s data). Calibration for uniaxial stress in the range $0 \leq e \leq 700\%$. Predictions for pure shear and biaxial stress.

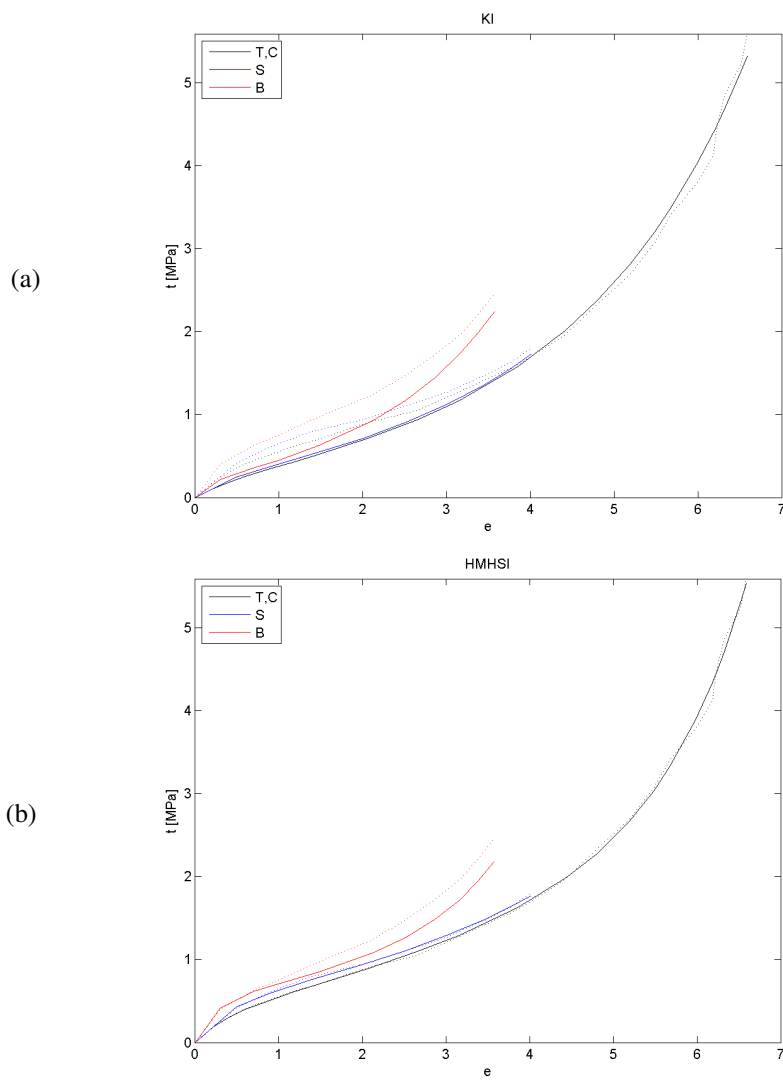


Figure 2. Natural Rubber (Treloar’s data). Calibration for uniaxial stress in the range $0 \leq e \leq 700\%$. (a) KI model; (b) HMHSI model.

5.2. Case Study: Natural Rubber – Small Deformations (NR55)

The same tests and selected models of section 4.1 were applied here for NR55 rubber in the range $0 \leq e \leq 100\%$. Figure 3 illustrates the good results obtained with the HMLSI model. It is worth to note that the PSI model didn't provide results with an agreement as good as it did the $0 \leq e \leq 700\%$ range.

The comparison of the HMLSI model with the KI model is shown in Fig.4, where the ability of the former in capturing the stiffness changes is evident.

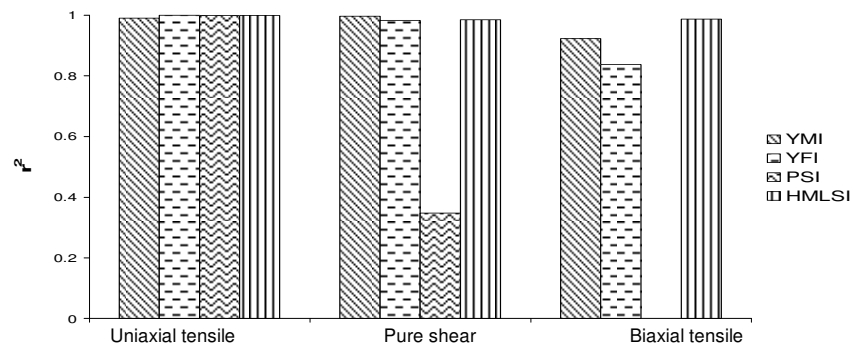


Figure 3. Natural Rubber (NR55 data). Calibration for uniaxial stress in the range $0 \leq e \leq 100\%$. Predictions for pure shear and biaxial stress.

5.3. Case Study: Silicon Rubber (MED4950)

The MED4950 silicon data (Meier *et al.*, 2003) was used again for calibrating all four models with the uniaxial testing in the range $0 \leq e \leq 600\%$. Figure 3 compares the results obtained for the selected models. Again, the HMHSI model provided a good performance, comparable only with the YMI model, but the latter didn't show similar performance with natural rubber (see section 4.1). Figure 6 shows that the biaxial prediction of the HMHSI model is superior to the one provided by the KI model.

6. CONCLUSIONS

This work summarizes a detailed comparison of 40 hyperelastic models concerning quality of the fit with experimental data and theoretical predictions for deformation modes other than the one used in the calibration. From that study, it was possible to identify, among all models studied, which ones presented better overall performance in characterizing elastomeric materials under small (100%) and large (700%) deformation ranges for three samples of incompressible materials. It was found that those containing power-law terms of the first strain invariant in their strain energy function were always among the best ones. Further investigation of the strain energy functions of the selected models showed that those containing e^{I_1} terms could represent more easily the rapid stiffness oscillation under small strains, while the ones including $\ln(I_2)$ terms were able to capture the characteristic stiffening at higher strains.

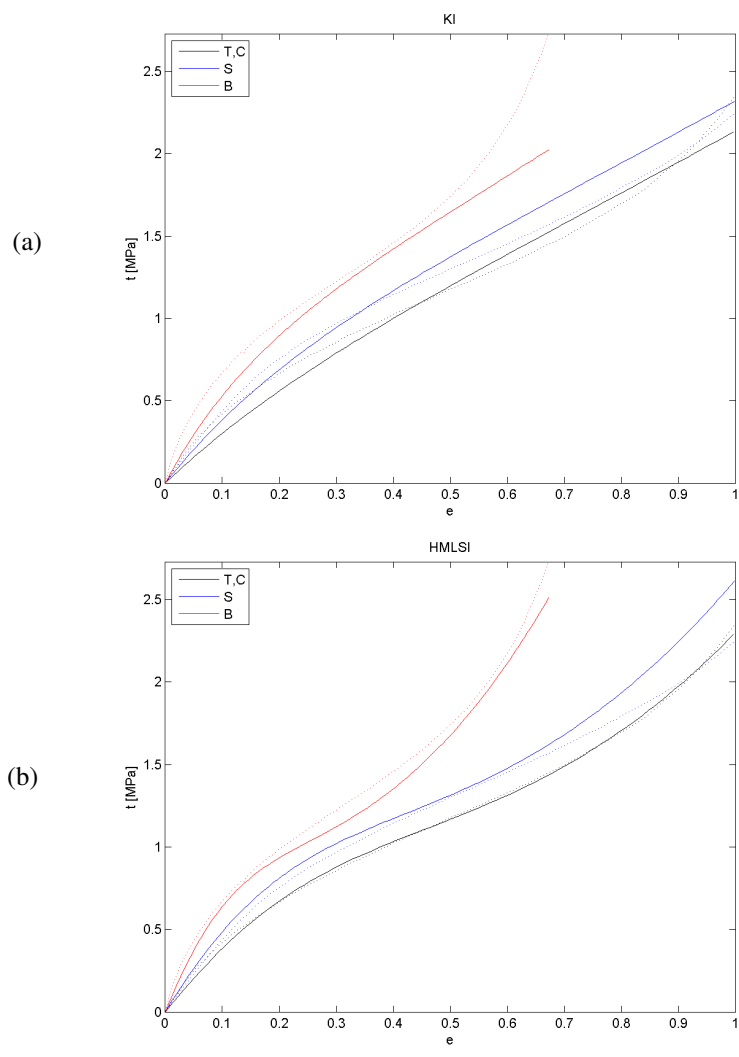


Figure 4. Natural Rubber (Treloar's data). Calibration for uniaxial stress in the range $0 \leq e \leq 100\%$. (a) KI model; (b) HMLSI model.

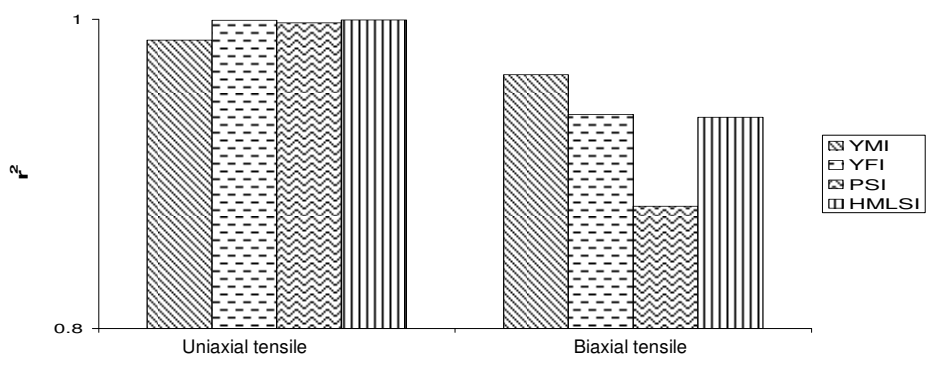


Figure 5. MED 4950 silicon. Calibration for uniaxial stress in the range $0 \leq e \leq 600\%$. Predictions for biaxial stress.

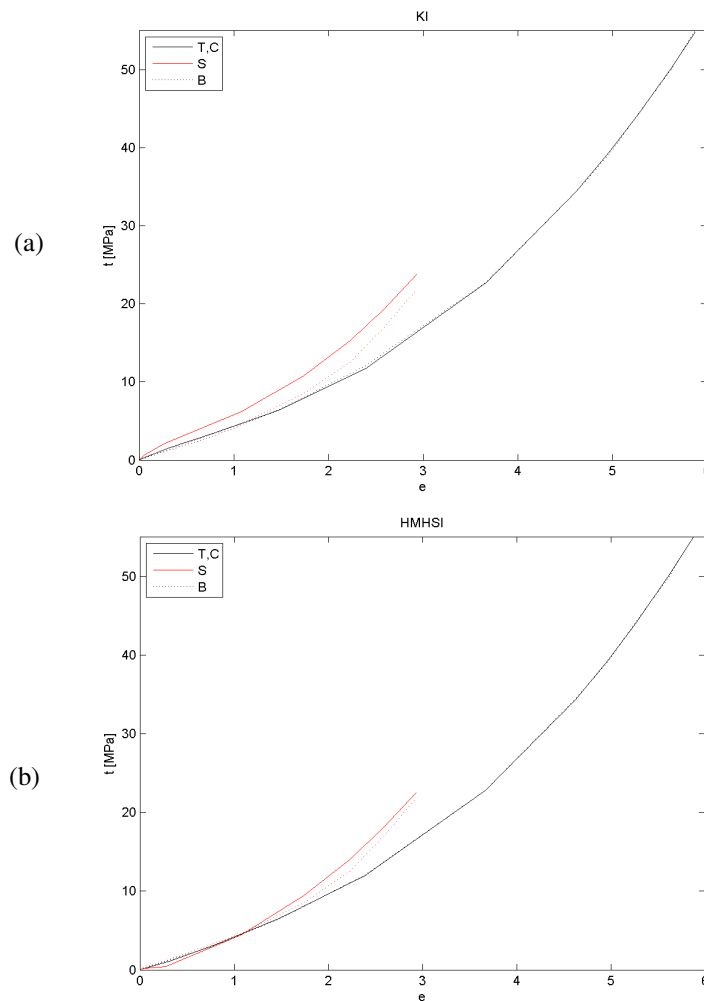


Figure 6. MED4950 silicon. Calibration for uniaxial stress in the range $0 \leq e \leq 600\%$. (a) KI model; (b) HMLSI model.

REFERENCES

- Amin, A.F.M.S., Alam, M.S., Okui, Y., An improved hyperelasticity relation in modeling viscoelasticity response of natural and high damping rubbers in compression: experiments, parameter identification and numerical verification, *Mech. Mater.* Vol.34, pp. 75–95, 2002.
- Arruda, E.M., Boyce, M.C., A three-dimensional constitutive model for the large stretch behavior of rubber elastic materials. *Journal of the mechanics and physics of solids*, Vol. 41, pp. 389-412.
- Bechir, H., Chevalier, L., Chaouche, M., Boufala, K., 2006, Hyperelastic constitutive model for rubber-like materials based on the first Seth strain measures invariant, *Eur. J. Mech. A/Solids*, vol.25, pp. 110–124, 1993.
- Boyce, M.C., Arruda, E.M., Constitutive models of rubber elasticity: a review. *Rubber Chemistry and Technology*, Vol. 73, n. 3, pp. 504-523, 2000.
- Davies, C.K.L., De, D.K., Thomas, A.G., Characterization of the behavior of rubber for engineering design purposes (1) Stress and strain relations, *Rubber chemistry and technology*, Vol. 67, pp. 716, 1994.
- Edwards, S.F., Vilgis, T.A., The effect of entanglements in rubber elasticity, *Polymer*, vol.27, pp.483-492, 1986.
- Fung, Y.C.B., Elasticity of soft tissues in sample elongation, *American Journal of Physiology*, Vol. 213, pp. 1532-1544, 1967.

- Gent, A.N., Thomas, A.G. J., *Polymer Science*, Vol. 28, pp. 625, 1958.
- Gent, A.N., A new constitutive relation for rubber, *Rubber chemistry and technology*, Vol. 69, pp. 59-61, 1996.
- Gent, A.N., Elastic Instabilities of inflated rubber shells, *Rubber chemistry and technology*, Vol. 72, pp. 263-268, 1999.
- Gregory, I.H., Muhr, A.H., Stephens, I.J., Engineering applications of rubber in simple extension, *Plastics, Rubber and Composites: Processing and Applications*, Vol. 26, pp. 118, 1997.
- Hart-Smith, L.J.. Elasticity parameters for finite deformation of rubber-like materials. *ZAMP* vol.17, pp.608–625, 1966.
- Hartmann, S., Neff, P., Polyconvexity of generalized polynomial-type hyperelastic strain functions for near-incompressibility, *International Journal of Solids and Structures*, Vol. 40, pp. 2767-2791, 2003.
- Horgan, C.O., Saccomandi, G., Constitutive models for atactic elastomers. *World Scientific* Singapore, pp. 281-293, 2004.
- Hoss, L., *Hyperelastic Constitutive Models for Incompressible Elastomers: Fitting, Performance Comparison and Proposal of a New Model*, M.Sc. thesis (in Portuguese), UFRGS, 2009.
- Humphrey, J.D., Continuum biomechanics of soft biological tissues, *Proc. R. Soc. Lond. A* 59, pp.1-44, 2003.
- Humphrey, J.D., Yin, F.C.P., On Constitutive relations and finite deformations of passive cardiac tissue: I. A pseudostrain energy function ASME, *Journal of Biomechanical Engineering*, Vol. 109, pp. 298-304, 1987.
- Jones, D., Treloar, L., The properties of rubber in pure homogeneous strain. *J. Phys. D: Appl. Phys.* V. 8, p. 1285-1304, 1975.
- Kilian, H.G., Equation of state of real networks. *Polymer*, Vol. 22, pp. 209-217, 1981.
- Knowles, J.K., The finite anti-plane shear field near the tip of a crack for a class of incompressible elastic solids, *International Journal of Fracture*, Vol.13, pp. 611-639, 1977.
- Marczak, R., Hoss, L. Gheller, J.J., *Caracterização de Elastômeros para Simulação Numérica*, Centro Tecnológico de Polímeros SENAI, São Leopoldo-RS, 2006.
- Martins, J.A.C., Pire, E.B., Salvado, R., Dinis, P.B., A numerical model of passive and active behavior of skeletal muscles, *Computer Methods in Applied Mechanics and Engineering*, Vol. 151, pp. 419-433, 1998.
- Meier P., Khader S., Preuß R., Dietrich J. and Voges D., Uniaxial and equi- biaxial tension tests of silicone elastomer, *Constitutive Models for Rubber III*, Busfield & Muhr (eds), Swets & Zeitlinger, Lisse, pp.99-106, 2003.
- Ogden, R.W., Large deformation isotropic elasticity – on the correlation of theory and experiment for incompressible rubber-like solids, *Proc. Roy. Soc. A*-326, pp. 565–584, 1972.
- Peng, S.T.J., Landel, R.F., Stored energy function and compressibility of compressible rubber-like materials under large strain, *Journal of Applied Physics*, Vol. 43, pp. 3064, 1972.
- Pucci, E., Saccomandi, G., A note on the Gent model for rubber-like materials, *Rubber chemistry and technology*, vol. 75, pp.839-851, 2002.
- Rivlin, R.S., Large elastic deformation of isotropic materials: I. Fundamental concepts. II. Some uniqueness theorem for pure homogeneous deformation, *Phil. Trans. R. Soc. A*-240, pp. 459-508, 1948.
- Rivlin, R.S., Saunders, D.W., Large elastic deformations of isotropic materials VII. Experiments on the deformation of rubber, *Phil. Trans. R. Soc. A*-243, pp. 251–288, 1951.
- Rozenwald, D. Modélisation thermomécanique des grandes déformations. *Application aux problèmes de mise a forme des métaux, des élastomeres et des structures mixtes métalelastomere*. PhD thesis, University of Liege, Liege, 1996.
- Takamizawa, K., Hayashi, K., Strain energy density function and uniform strain hypothesis for arterial mechanics, *Journal of Biomechanics*, Vol. 20, pp. 7-17, 1987.
- Treloar, L.R.G.. Stress–strain data for vulcanized rubber under various types of deformation. *Trans. Faraday Soc.* 40, pp. 59–70, 1944.

- Treloar, L., *The Physics of Rubber Elasticity*, Oxford: Clarendon Press, 1975.
- Veronda, D.R., Westmann, R.A., Mechanical characterization of skin-finite deformations, *Journal of Biomechanics*, Vol. 3, pp. 111-124, 1970.
- Yamashita, Y., Kawabata, S., Approximated form of the strain energy-density function of carbon black filled rubbers for industrial application, *International Polymer Science Technology*, Vol. 20 (2), pp. 52-64, 1993.
- Yeoh, O.H., Characterization of elastic properties of carbon black filled rubber vulcanizates, *Rubber chemistry and technology*, Vol. 63, pp. 792-805, 1990.
- Yeoh, O.H., Some forms of the strain energy function for rubber, *Rubber chemistry and technology*, Vol. 66, pp. 754-771, 1993.
- Yeoh, O.H., Fleming, P.H., A new attempt to reconcile the statistical and phenomenological theories of rubber elasticity, *Journal of Polymer Science, B: Polymer Physics*, Vol. 35, pp. 1919-1931, 1997.